V.97
1980

T.A.Vsevolozskaya

THE OPTIMISATION AND EFFICIENCY OF ANTIPROTON PRODUCTION WITHIN A FIXED ACCEPTANCE
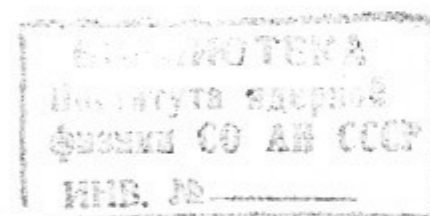
THE OPTIMISATION AND EFFICIENCY OF ANTIPROTON
PRODUCTION WITHIN A FIXED ACCEPTANCE

T.A.Vsevolozskaya

Institute of Nuclear Physics
630090, Novosibirsk 90, USSR

Abstract

The study of optimum conditions of antiproton production
within a fixed phase volume - the acceptance of antiproton
accumulator or another device, is performed to determine the
requirements for optical systems, used for proton focusing
onto the target and antiproton collection. Analytical evalua-
tion of particle capture efficiency is carried out and compa-
red to computer simulation results. The possibility to increa-
se the capture efficiency by means of antiproton focusing wi-
thin the target is considered on the examples of a target
with current, providing the distributed focusing through the
target length, and a target with concentrated focusing, carri-
ed out with lenses placed between target sections.

Antiproton emittance and optimum
targetry conditions

The optimisation of antiproton production inside a fixed phase volume – the acceptance of a storage ring or another device – consists in matching of the acceptance form to a particle distribution in phase space by optimum choice of the target and incident proton beam parameters to provide the high particle density inside the acceptance.

To find the antiproton distribution function in a first approximation one can neglect the elastic nuclear and multiple scattering of protons and antiprotons, the angular spread in the proton beam, and ionization losses of energy in comparison to the production angle and momentum spread of the antiprotons.

The equations determing the distribution function (the kinetic equations) of the antiprotons produced by incident protons interacting in a target, are in this approximation

$$\frac{\partial \bar{P}}{\partial z} + \theta \frac{\partial \bar{P}}{\partial r} = P(r,z) \cdot n_o \frac{d^2 \delta}{dp d\theta} - \delta_{in} n_o \bar{P}$$

$$\frac{\partial P}{\partial z} = -\delta_{in} n_o P$$

(1)

where $P(r,z)$ and $\bar{P}(r, \theta, z, p)$ are the proton and antiproton distribution functions, δ is the cross section of antiproton production, δ_{in} and δ_{in} are the proton and antiproton absorption cross sections , n_o is nuclear density in the target. From the second equation it follows $P(r,z) = P_o(r) e^{-z/\lambda}$, where $P_o(r)$ is the proton distribution across the incident proton beam, $\lambda = \frac{1}{\delta_{in} n_o}$ – the proton absorption length, and so the equation for $\bar{P}(r, \theta, z, p)$ is

$$\frac{\partial \bar{P}}{\partial z} + \theta \frac{\partial P}{\partial r} = P_o(r) e^{-z/\lambda} \cdot n_o \frac{d^2 \delta}{dp d\theta} - \delta_{in} n_o \bar{P}$$

(2)

After the integration of (2) over transverse phase space with the condition that $\bar{P}(r, \theta, z, p) \to 0$ at $r, tg\theta \to 0$, we have the equation, determing the antiproton yield dependen-

3

ce on the position z along the target $(0 \leq z \leq L)$:

$$\frac{d}{dz}\left(\frac{d\bar{N}}{dp}\right) = N_0\, e^{-z/\lambda}\, n_0\, \frac{d\bar{\delta}}{dp} - \bar{\delta}_{in}\, n_0\, \frac{d\bar{N}}{dp}$$

which gives:

$$\frac{d\bar{N}}{dp} = N_0 \frac{d\bar{\delta}}{dp} \cdot \frac{e^{-\delta_{in} n_0 z} - e^{-\bar{\delta}_{in} n_0 z}}{\bar{\delta}_{in} - \delta_{in}} \underset{\bar{\delta}_{in} = \delta_{in}}{=} N_0 \frac{1}{\delta_{in}} \cdot \frac{d\bar{\delta}}{dp} \frac{z}{\lambda} e^{-\frac{z}{\lambda}}, \quad (3)$$

where N_0 is the number of incident protons. The maximum value of $\frac{d\bar{N}}{dp}$ occurs at $z = z_m = \frac{\ln(\bar{\delta}_{in}/\delta_{in})}{n_0(\bar{\delta}_{in} - \delta_{in})}$. Because $\bar{\delta}_{in} \cong \delta_{in}$ one has $z_m \cong \lambda$, and $\left(\frac{d\bar{N}}{dp}\right)_{max} \cong \frac{N_0 n_0}{e} \frac{d\bar{\delta}}{dp}$.

If before integration of (2) we multiply it by r^2, $r\theta$ and θ^2 in turn there will be the system of equations determining respectively the mean values $\langle r^2 \rangle$, $\langle r\theta \rangle$ and $\langle \theta^2 \rangle$ in dependence on z:

$$\frac{\partial}{\partial z}\left(\langle r^2 \rangle \frac{d\bar{N}}{dp}\right) - 2\langle r\theta \rangle \frac{d\bar{N}}{dp} = N_0 n_0 \frac{d\bar{\delta}}{dp} e^{\frac{z}{\lambda}} \langle r_0^2 \rangle - \bar{\delta}_{in} n_0 \langle r^2 \rangle \frac{d\bar{N}}{dp}$$

$$\frac{\partial}{\partial z}\left(\langle r\theta \rangle \frac{d\bar{N}}{dp}\right) - \langle \theta^2 \rangle \frac{d\bar{N}}{dp} = -\bar{\delta}_{in} n_0 \langle r\theta \rangle \frac{d\bar{N}}{dp} \qquad (4)$$

$$\frac{\partial}{\partial z}\left(\langle \theta^2 \rangle \frac{d\bar{N}}{dp}\right) = N_0 n_0 \frac{d\bar{\delta}}{dp} e^{\frac{z}{\lambda}} \langle \theta_0^2 \rangle - \bar{\delta}_{in} n_0 \langle \theta^2 \rangle \frac{d\bar{N}}{dp}$$

where θ_0 and r_0 — denote the angle and coordinate of antiproton production. Using (3) the system is easily solved. For small difference between $\bar{\delta}_{in}$ and δ_{in} we have

$$\langle r^2 \rangle = \langle r_0^2 \rangle + \frac{z^2 \langle \theta_0^2 \rangle}{3}\left(1 - z n_0 \frac{\bar{\delta}_{in} - \delta_{in}}{4} + \cdots\right)$$

$$\langle r\theta \rangle = \frac{z \langle \theta_0^2 \rangle}{2}\left(1 - z n_0 \frac{\bar{\delta}_{in} - \delta_{in}}{6} + \cdots\right)$$

$$\langle \theta^2 \rangle = \langle \theta_0^2 \rangle$$

The values of the $\langle r^2 \rangle$, $\langle r\theta \rangle$ and $\langle \theta^2 \rangle$ determine the effective emittance of the antiproton beam $\varepsilon_{\bar{p}}$ as $\varepsilon_{\bar{p}} = \sqrt{\langle r^2 \rangle \langle \theta^2 \rangle - \langle r\theta \rangle^2}$, its envelope function $\beta_{\bar{p}}$ as $\beta_{\bar{p}} = \frac{\langle r^2 \rangle}{\varepsilon}$, the distance to the beam waist from the target exit

as $\Delta z = -\frac{\langle r\theta \rangle}{\langle \theta^2 \rangle}$, and the value of $\beta_{\bar{p}}$ in it as $\beta_{\bar{p},min} = \frac{\varepsilon_{\bar{p}}}{\langle \theta^2 \rangle}$. For an extremely thin proton beam $\left(\langle r_0^2 \rangle \ll \frac{z^2 \langle \theta_0^2 \rangle}{12}\right)$ and $\bar{\delta}_{in} = \delta_{in}$ these are $\varepsilon_{\bar{p}} = \frac{z \langle \theta_0^2 \rangle}{2\sqrt{3}}$, $\Delta z = -\frac{z}{2}$, $\beta_{\bar{p},min} = \frac{z}{2\sqrt{3}}$ (5).
The emittance value at a target length corresponding to the maximum antiproton yield, i.e. $z \cong \lambda$, can be taken as an characteristic emittance ε_0 of an antiproton production for chosen antiproton momentum and target material. The linear dependence of $\varepsilon_{\bar{p}}$ on target length whereas the time of antiproton yield is proportional to $z\, e^{-z/\lambda}$ shows that the optimum z is considerably smaller than λ if the antiprotons are captured into the acceptance much smaller than ε_0.

To determine the production angle it is convenient to use the thermodynamic description of the transverse momentum distribution $\omega(p_\perp)\, dp_\perp^2 \propto \sqrt{m_\perp} \exp\left(-\frac{m_\perp}{T}\right)$ (6), which agrees well enough with experimental data at small value of $p_\perp$ $(p_\perp^2 \ll m^2)$ when the temperature T is taken of the order of π-meson's mass, $T \cong m_\pi$. The $m_\perp$ in (6) is transverse mass $m_\perp = \sqrt{m^2 + p_\perp^2}$. The angular distribution which follows from (6) is nearly Gaussian with mean square of angle $\langle \theta_0^2 \rangle \cong \frac{2mT}{p^2} \cong \frac{2m m_\pi}{p^2}$, where m and p are the antiproton mass and momentum. So the production emittance for the antiprotons with momentum p is $\varepsilon_0 \cong \frac{m m_\pi \lambda}{\sqrt{3}\, p^2}$.

The equation which determines the number of antiprotons N_ε, captured into the acceptance ε, is obtained after an integration of (2) over angles and transverse coordinates inside the acceptance. Then one easily sees that on the left side there remains the term $\frac{\partial}{\partial z}\int^\varepsilon \bar{P}\, d^2r\, dO = \frac{dN_\varepsilon}{dz}$ only agreement with conservation of phase space by free particle motion. So we have

$$\frac{dN_\varepsilon}{dz} = n_0\, e^{-z/\lambda} \frac{\varepsilon}{\Delta p} \int^\varepsilon P_0(r) \frac{d^2\bar{\delta}}{dp\, dO} \cdot d^2r\, dO - \bar{\delta}_{in} n_0 N_\varepsilon \qquad (7)$$

where Δp is a momentum bite captured.

To determine the sphere of integration in the right side of (7) we must use the dependence of acceptance β- and α- or γ- and α- functions on longitudinal target coordinate z. The second couple is preferable because the γ-function has a constant value in a drift determined by the value of

β - function in a waist β_{min} as $\gamma = \frac{1}{\beta_{min}}$. The   of acceptance has, evidently, to be zero at the waist of the antiproton beam, i.e. in the target centre by $\bar{\delta}_{in} = \delta_{in}$. Thus α is related to the γ and β_{min} as $\alpha = -\gamma \left(z - \frac{L}{2}\right) = -\frac{1}{\beta_{min}} \left(z - \frac{L}{2}\right)$, where L is the target length.

Let the proton beam have a radius r_0 less than the coordinate size of the acceptance in its minimum, $r_0 < \sqrt{\frac{\varepsilon}{\gamma}} = \sqrt{\varepsilon \beta_{min}}$. Then for Gaussian distribution of antiproton production angles, $\frac{d^2\bar{\delta}}{dp\,dO} = \frac{d\bar{\delta}}{dp} \cdot \frac{exp(-\theta^2/\langle\theta_0^2\rangle)}{\pi \langle \theta_0^2 \rangle}$, and $\bar{\delta}_{in} \cong \delta_{in}$ we have

$$N_\varepsilon = n_0 \frac{d\bar{\delta}}{dp} e^{-\frac{L}{\lambda}} \int_0^L \int_0^{r_0} \int_0^{2\pi} erf \frac{\vartheta_x}{\sqrt{\langle\theta_0^2\rangle}} \; erf \frac{\vartheta_y}{\sqrt{\langle\theta_0^2\rangle}} \; P_0(r) r\,dr\,d\varphi\,dz \quad (8)$$

where $\vartheta_x = \left[\frac{zx\gamma}{2}\theta^2 + \sqrt{\varepsilon\gamma\left(1 + \frac{z^2\gamma^2}{4}\right) - x^2\gamma^2}\right] / \left(1 + \frac{z^2\gamma^2}{4}\right)$ and the same for ϑ_y with $y = r \sin\varphi$ replacing the $x = r\cos\varphi$. For infinitely thin proton beam, $P_0(r) = N_0 \delta(x)\delta(y) = \frac{N_0}{2\pi r}\delta(r)$, the expression (8) is simplified to

$$N_\varepsilon \underset{r_0=0}{=} N_0 n_0 \frac{d\bar{\delta}}{dp} e^{-\frac{L}{\lambda}} \Delta p \int_0^L \left[erf \sqrt{\frac{\varepsilon\gamma}{\langle\theta_0^2\rangle\left(1 + \frac{z^2\gamma^2}{4}\right)}} \right]^2 dz \quad (9)$$

In the case where the   range of angles captured is small compared to the range produced, $\varepsilon\gamma \ll \langle\theta_0^2\rangle$, the expression under the integral can be expaned in a series, and taking into account only the first term we have

$$N_\varepsilon \underset{r_0=0}{\cong} N_0 \cdot \Delta p \frac{1}{\delta_{in}} \frac{d\bar{\delta}}{dp} \cdot \frac{8\varepsilon e^{-L/\lambda}}{\pi\lambda\langle\theta_0^2\rangle} \; arc\,tg \frac{L\gamma}{2} \quad (10)$$

If we set the value of γ of the acceptance at the target equal to that of the antiproton beam, $\gamma = \frac{2\sqrt{3}}{L}$, which is close to optimum for the acceptance not too small compared to ε_0 , we have

$$N_\varepsilon = \frac{N_0}{\delta_{in}} \cdot \Delta p \cdot \frac{d\bar{\delta}}{dp} \cdot \frac{8}{3} \cdot \frac{\varepsilon e^{-\frac{L}{\lambda}}}{\lambda\langle\theta_0^2\rangle} \quad (11)$$

Here we see the exponential decrease of N_ε with target length when $L = \frac{2\sqrt{3}}{\gamma} \gg 2\sqrt{3}\frac{\varepsilon}{\langle\theta_0^2\rangle}$.

To find the optimal target length L_{opt} by the accepted dependence of γ on L we have to solve the equation $\frac{\partial N_\varepsilon}{\partial L} = 0$. Taking into account two terms of the series in the right side of (9) we have

$$L_{opt} \cong 1.28\lambda \sqrt{\frac{\varepsilon}{\lambda\langle\theta_0^2\rangle}} \left(1 + 0.64\sqrt{\frac{\varepsilon}{\lambda\langle\theta_0^2\rangle}} + \cdots \right) \quad (12)$$

$$N_\varepsilon(L_{opt}) \cong \frac{N_0}{\delta_{in}} \cdot \frac{d\bar{\delta}}{dp} \cdot \Delta p \cdot \frac{8}{3} \frac{\varepsilon \; exp(-L_{opt}/\lambda)}{\langle\theta_0^2\rangle(\lambda + L_{opt})}$$

For finite radius of a proton beam and uniform particle distribution in it the expression for L_{opt} is $L_{opt} = \sqrt{R}\left(1 + \frac{1}{2}\sqrt{R} + \cdots\right)$ (13), where

$$R = 1.65\left(\frac{\varepsilon}{\lambda\langle\theta_0^2\rangle} + \frac{3}{8}\frac{r_0^2}{\varepsilon\lambda}\right)$$

For very small values of acceptance the $\gamma = \frac{2\sqrt{3}}{L}$ may appear to be far from optimum. To optimize it together with L we have to solve the equation $\frac{\partial N_\varepsilon}{\partial \gamma} = 0$ together with $\frac{\partial N_\varepsilon}{\partial L} = 0$. This solution leads to the next expressions for γ_{opt} , L_{opt} , and $N_{\varepsilon,max}$:

$$\beta_{opt} \cong \frac{1}{\gamma_{opt}} = \frac{\lambda}{\pi} \cdot \frac{R^{2/3}}{1 - \frac{4}{3\pi}R^{1/3}}$$

$$L_{opt} \cong \frac{2\lambda}{\pi} \cdot \frac{R^{1/3}}{\left(1 - \frac{4}{3\pi}R^{1/3}\right)^2} \quad (14)$$

$$N_{\varepsilon,max} \cong \frac{N_0}{\delta_{in}} \cdot \frac{d\bar{\delta}}{dp} \cdot \Delta p \cdot \frac{4\varepsilon \; e^{-L_{opt}/\lambda}}{\langle\theta_0^2\rangle\lambda}\left(1 - \frac{4}{3\pi}R^{1/3}\right)^3$$

At the limit $R \to 0$ the value of $N_{\varepsilon,max}$ (Eq. 14) differs from N_ε (Eq. 12) by a factor of 1.5 times, but already at $R \sim 10^{-2}$ the difference is less than 10%. The thin proton beam condition $r_0^2 \ll \frac{8}{3} \cdot \frac{\varepsilon^2}{\langle\theta_0^2\rangle}$, following from (13) and (14), is sufficiently more strict than obtained by the antiproton beam emittance definition (see (5)). This difference is due to the strong ingomogeneity of the antiproton distribution at small

6

7

angles and coordinates, which does not influence sufficiently on the integral characteristics of whole distribution.

Analytical estimates of the optimum values of capture efficiency, collection angle, target length and of the efficiency dependence on proton beam size are well consistent with results of computer similation (see Fig. 1-4), in which the multiple and elastic nuclear scattering of protons and antiprotons, the difference in their absorption lengths, the angular spread and real coordinate distribution in proton beam were taken into account. The capture efficiency is characterized with a function F equal to the ratio of the number of antiprotons captured to the number of would be produced in whole transverse phase space by interaction of all primary protons without antiproton absorption. The F equals to 1 in the case of an infinitely large acceptance, long and thin target and thin proton beam. The number of antiprotons captured is determined with F as

$$ N_E = N_o \cdot \frac{d\bar{\sigma}}{dp} \cdot \frac{\Delta p}{\sigma_{in}} \cdot F = N_o \cdot \frac{d^2\bar{\sigma}}{dpd\Omega} \cdot \frac{\Delta p}{\sigma_{in}} \cdot \pi \langle \theta_o^2 \rangle \cdot F \qquad (15) $$

In Fig. 1 it is shown the F dependence on an acceptance value at optimum values of acceptance γ-function, at Fig. 2 - on a mean square of proton beam radious, which for the uniform particle distribution inside a cylinder $r_o \leqslant r_{max}$, postulated in analytical evaluation, is $\langle r_o^2 \rangle = \frac{1}{2} \cdot r_{max}^2$. In computer simulation the proton distribution across the beam is taken for Gaussian. Difference in curves in Fig. 2 at very small $\langle r_o^2 \rangle$ is due to influence of angular spread in the proton beam, when this spread, increasing with beam size decrease at a finite value of beam emittance, becomes of the order of or more than the range of angles captured. The F dependence on target length (Fig. 3) is shown for target with very large cross section and for thin one with a cross section of the order of proton beam cross section. At a large L the thin target gives a marked gain due to the smaller absorption of antiprotons, but the difference in F at optimum target lengths

does not exceed 15%.

The optimisation of antiproton capture into an accumulator includes the optimum choice of injection momentum. This choice is determined by the energy dependence of production cross-section and by the accumulation scheme. In the case of antiproton deceleration before cooling, as in the INP-IHEP project /1/, the maximum accumulation rate is achieved by the injection at a momentum, corresponding to the maximum of $p\frac{d^3\bar{\sigma}}{dp^3}$ the cross section of antiproton production within a phase volume element $\frac{d^3p}{p}$, which is conserved at the adiabatic particle deceleration. This element contains in a product $p^2\varepsilon\frac{\Delta p}{p}$ in eq. (12) (or (14)), when as a result of the relation $\frac{d\bar{\sigma}}{dp} = \pi \langle \theta_o^2 \rangle \frac{d^2\bar{\sigma}}{dpd\Omega} \big|_{\theta=0^o}$ use it turns into

$$ N_E = N_o \frac{1}{\sigma_{in}} \cdot p\frac{d^3\bar{\sigma}}{dp^3} \bigg|_{\theta=0^o} \cdot \frac{8\pi}{3} \cdot \frac{e^{-L_{opt}/\lambda}}{\lambda + L_{opt}} \cdot p^2 \varepsilon \frac{\Delta p}{p} $$

The dependence of $p\frac{d^3\bar{\sigma}}{dp^3}$ on p for proton energy E_o = 70 GeV is shown in Fig. 5. The solid line, plotted with the use of the old IHEP experimental data extrapolated to low momenta under the symmetry of the invariant cross-section versus c.m.s. rapidity, shows that the maximum of $p\frac{d^3\bar{\sigma}}{dp^3}$ lies near 5.5 GeV/c. As the more recent data compilation shows the maximum is rather shifted down to 4,5 GeV/c. In case of the stochastic cooling of the antiproton momentum spread before the deceleration, as in the FNAL project /2/, the cross-section $\frac{d^2\bar{\sigma}}{dpd\Omega}$ has to be maximized.

Antiproton collection

Antiproton collection from the target requires an optic system with a large angular acceptance and a short focal distance. The optimum collection angle ϑ_c is determined by values of the acceptance and its γ - function at the target as $\vartheta_c = \sqrt{\varepsilon\gamma}$. For $\gamma = \gamma_p$ (eq. 5), $r_o \cong 0$ and $L = L_{opt}$ (eq. 12) it is $\vartheta_c \cong 1,65 \left(\frac{\varepsilon\langle\theta^2\rangle}{\lambda} \right)^{1/4}$. The restriction of focal distance does not directly follow from the above consideration of optimum tar-

getry conditions. It arises from   the beam emittance
distortion in the lens due to aberration, particle scattering
and so on. And it is most   strict in a case of small accep-
tance, because, thanks to sharp maximum of antiproton density
at the center of emittance, the aberration increase of partic-
le angles or coordinates does not lead to the marked reduction
of capture efficiency when this increase is small compared to
the corresponding dimension of acceptance only. Thus the rest-
riction of aberration (or scattering) angle α_{ab}, being also
the restriction of lens focal distance f, is:

$$\langle \alpha_{ab}^2 \rangle < \frac{\varepsilon}{\beta} \cong \frac{\varepsilon \beta_0}{f^2} \qquad (16)$$

where ε is the value of acceptance, β- its beta-function in
the lens, related to that in a particle source β_0 as $\beta = \beta_0 + \frac{f^2}{\beta_0}$.
Figure 4 shows the efficiency of antiproton collection with
different optic systems - lithium lenses /3/ with focal dis-
tances f = 10 cm and 20 cm, parabolic lenses (magnetic horns)
with f = 20 cm, made of berillium and aluminium, and quadru-
pole triplet /4/ - compared with ideal focusing for the FNAL
project parameters ($\varepsilon = 5 \cdot 10^{-6} m.rad$, $pc = 4.5\,GeV$, $\frac{\Delta p}{p} = \pm 2\%$).
In the case of lithium and parabolic lenses the capture effici-
ency reduction is mainly due to nuclear absorption and multip-
le scattering, in the case of triplet - to chromatic aberrati-
on /5/. The lithium lenses considered /3/ have 6 cm length l,
0.25 cm (for f = 10 cm) and 0.5 cm (for f = 20 cm) end be-
rillium flanges thicknesses, 1 cm and 2 cm aperture diameters,
140 KOe maximum field. Under a focusing, characterized with
particle oscillation frequency ω, the multiple scattering in
lithium results in the mean square angle $\langle \theta^2 \rangle_{li}$ less by a fac-
tor of $\frac{1}{2}\left(1 + \frac{\sin 2\omega l}{2\omega l}\right)$ than $\langle \theta^2 \rangle_{li}$ without focusing. When
f = 10 cm, the angle of scattering in lithium and berillium
flanges, $\sqrt{\langle \theta^2 \rangle} = 7 \cdot 10^{-4} rad$, meets the condition (16) and los-
ses in capture efficiency scarcely exceed nuclear losses. At
f = 20 cm the multiple scattering leads to a marked loss in
capture efficiency.

Antiproton focusing within the target

As it is seen from the first item, the effective trans-
verse antiproton beam emittance on the condition of infinitely
thin proton beam arises from the target length - the spread of
longitudinal production coordinate z turns into transverse
coordinate r spread in a beam cross section in accordance
with dependence (the linear one) of r on z. Full fourdimen-
sional transverse beam phase volume remains zero because of
zero value of particle φ - velocities. Changing the dependen-
ce r on z one can decrease the transverse antiproton beam
emittance and, hence, increase the particle density inside the
acceptance.

Antiproton focusing with magnetic field of a current passing
through the target along the beam axis /6/, at high enough
current value, eliminates the emittance dependence on target
length. It allows to extend the target length up to the value
corresponding to the maximum antiproton yield. The antiproton
beam emittance in this case is determined by the field gradi-
ent only and, in principle, can be done small enough to provi-
de high capture efficiency. The maximum value of F is determi-
ned by nuclear target efficiency, i.e. $F \cong e^{-1}$ at $\delta_{in} = \delta_{in}$,
if proton defocusing in the target may be neglected. To take
the antiproton focusing into account in kinetic equations, we
have to add the term $- \omega^2 r \frac{\partial \bar{p}}{\partial \theta}$ to the left hand side of the
first equation of system (1). On the left hand sides of the
second and third equations of system (4) there appear the terms
$\omega^2 \langle r^2 \rangle \frac{dN}{dp}$ and $2\omega^2 \langle r\theta \rangle \frac{dN}{dp}$, respectively. At $\delta_{in} = \delta_{in}$,
taking into account (3), one obtains

$$\langle \theta^2 \rangle = \frac{\langle \theta_0^2 \rangle}{2} \left(1 + \frac{\sin 2\omega z}{2\omega z}\right)$$

$$\langle r^2 \rangle = \frac{\langle \theta_0^2 \rangle}{2\omega^2} \left(1 - \frac{\sin 2\omega z}{2\omega z}\right) \qquad (17)$$

$$\langle r\theta \rangle = \frac{\langle \theta_0^2 \rangle}{4\omega^2 z} \left(1 - \cos 2\omega z\right)$$

where $\omega = \sqrt{\frac{qG}{pc}}$ — the frequency of antiproton oscillation in a field inside the target, G — field gradient, p and q — antiproton momentum and charge. The effective emittance of antiproton beam is

$$\varepsilon_{\bar{p}} = \frac{\langle \theta_0^2 \rangle}{2\omega} \sqrt{1 - \frac{\sin^2 \omega z}{\omega^2 z^2}}$$

At fixed ω the antiproton emittance achieves the value close to the limit $\lim_{z \to \infty} \varepsilon_{\bar{p}} = \frac{\langle \theta_0^2 \rangle}{2\omega}$ already at $z \cong \frac{\pi}{2}$, but this value slightly differs from the emittance for a target of optimum length without field. It means that to obtain the marked gain in capture efficiency, the field gradient has to be large enough to enable the equality $\omega z = \frac{\pi}{2}$ at a z less than the optimum target length without field L_{opt}, determined by eq. (12) (or eq. (14) for very small ε compared to $\lambda \langle \theta_0^2 \rangle$). So we have $\omega > \frac{\pi}{2 L_{opt}} \cong \sqrt{\frac{\langle \theta_0^2 \rangle}{\varepsilon \lambda}}$ and $G > \frac{2 m m_{\bar{p}} c^3}{q p \varepsilon \lambda}$. For the INP-IHEP antiproton source project /1/ ($\varepsilon = 6 \cdot 10^{-5}$ mrad, $pc = 5.5$ GeV) it means $G > 0.27$ MOe/mm. The estimate for the FNAL project with L_{opt} determined in eq. (14) gives $G > 2$ MOe/mm.

At $\omega L \gg \frac{\pi}{2}$, infinitely thin proton beam, and $\delta_{in} \cong \delta_{in}$ the capture efficiency into acceptance ε is found as $F = e^{-1} \cdot \left[erf \sqrt{\frac{\varepsilon \omega}{\langle \theta_0^2 \rangle}} \right]^2$ (18), but the applicibility of this expression is restricted by proton defocusing in the target.

Effect of proton defocusing on antiproton capture efficiency F for the FNAL and IHEP beam parameters is clearly seen (Fig. 6 and 7) from the comparison of F dependence on field gradient G at different values of proton energy E_0 and of beam emittance ε_p ($\varepsilon_p \propto \frac{1}{E_0}$) and β - function in the target β_p ($\beta_p \propto E_0$), accordingly. Figure 6b shows the dependence of optimum target length L_{opt} on G in the case of Fig. 6a. Decrease of L_{opt} with an increase of G above some value also evidences the effect of proton defocusing.

Antiproton focusing inside the target leads to some decrease of angular spread at target exit (see eq. (17)). At a fixed value of emittance $\varepsilon_{\bar{p}}$ it means the increase of beam β - function in the waist, $\beta_0 = \frac{\varepsilon_{\bar{p}}}{\langle \theta^2 \rangle}$, as compared to its

value in the case of target without field at the same value of $\varepsilon_{\bar{p}}$.

This increase is maximum at $\omega L \cong 0.7 \pi$ and is characterized by a factor of about 2.5. Hence the increase of beta-function of acceptance β without losses in phase particle density does not exceed significantly the factor 2 or 3. In the case of figure 6 the optimum β of acceptance is maximum and equals ~ 7 mm at $G \sim 2$ MOe/mm. At $\omega L \gg \frac{\pi}{2}$, $\beta \cong \omega^{-1}$.

Magnetic field with gradient of several MOe/mm requires very high current density in the target ($j \left(\frac{A}{mm^2} \right) = \frac{1}{2\pi} G \left(\frac{Oe}{mm} \right)$), accompanied with very high density of resistive energy deposition. It leads to thermal distortion of the target for a very short time which can be less than the proton spill duration. With taking into account the alteration of target material electro-conductivity δ as $\delta = \frac{\delta_0}{1 + \beta Q}$ /7/, the time of target heating up to the melting temperature T_{melt} is determined as follows:

$$t = \frac{\delta_0 \ln (1 + \bar{\alpha} \cdot T_{melt})}{\beta^2 \bar{j}^2} \tag{18}$$

where δ_0 is the initial value of δ, β - its thermal coefficient, nearly constant in the temperature interval from $20°C$ to T_{melt}, $\bar{\alpha}$ - the mean value of temperature coefficient, Q - the density of deposited energy, $\bar{j}^2$ - mean square value of current density. For tangsten target ($\delta_0 = (5.5 \cdot 10^{-5} \text{ Ohm} \cdot mm)^{-1}$, $\beta = 1.8 (J/mm^3)^{-1}$, $\bar{\alpha} = 5.8 \cdot 10^{-3} (°C)^{-1}$, $T_{melt} = 3380°C$) the heating time is

$$t, s = \frac{1.2 \cdot 10^{-6}}{(G, MOe/mm)^2} \tag{19}$$

Deposition of energy for melting increases this time not more than by 15%, and so the target distortion under field gradient of several MOe/mm begins sooner than in a microsecond. It agrees very well with the results of experimental study of target behaviour at such fields, carried out in the INP /6,8/ in

1968. So, the short "life-time" of the target narrows the applicibility range of current targets despite of all theire attractivity.

Another way to increase phase density of antiprotons inside the acceptance /9/ consists in replacing the target by several short ones with strong lenses placed between them to focuse the antiprotons from one target to another. In this case the trajectories of antiprotons produced in different targets coincide and the whole beam emittance does not exceed the emittance from one short target. The optimum value of summary target length $L_{opt}^{(N)}$ depends on the number of targets N as

$$L_{opt}^{(N)} = N \cdot \ell_i^{(N)} \cong \sqrt{RN} \left(1 + \frac{1}{2}\sqrt{RN} + \cdots\right)$$
$$i = 1,2,3,\ldots,N$$

where R has the same value as in eq. (13). The value of beam γ - function is determined by the length of one target $\ell_i^{(N)}$, $\gamma_{\bar{p}} = \frac{2\sqrt{3}}{\ell_i^{(N)}} \sim \frac{2\sqrt{3}}{\lambda\sqrt{R}}\sqrt{N}$. Thus the acceptance γ , equal to $\gamma_{\bar{p}}$, and solid collection angle $\pi\vartheta_c^2 = \pi\varepsilon\gamma$ increase with N as $\sqrt{N}$ together with the same increase of summary target length, and so the capture efficiency increases approximately as N :

$$F \doteq \frac{8}{3} N \frac{\varepsilon}{\langle\theta_0^2\rangle} \cdot \frac{exp\left(-L_{opt}^{(N)}/\lambda\right)}{L_{opt}^{(N)} + \lambda} \qquad (20)$$

The transformation of expressions (14) to the case of N targets also consists in replacing R by product RN and in multiplying the expressions for γ opt. and F by N .

The lenses between targets must have the shortest focal distances to minimize the aberration effect and the length of whole system, which determines the value of proton beam β - function at the targets. For lithium lens, occupying all the distance between targets d , the value of d is related to maximum field in a lens as $H_{max} \cdot d = \pi\sqrt{\varepsilon\gamma}\,\frac{pc}{q}$. For $H_{max} \sim 300\,KOe$ using the dependence of optimum $\gamma = \gamma_{\bar{p}}$ on ε one obtains $d\,(cm) = 0.5\left[pc\,(GeV)\right]^{3/2} \cdot \left[N \cdot \varepsilon\,(cm.rad)\right]^{1/4}$.

14

For practically interesting values of ε and p the value of d can not be done significantly shorter than 10 cm, and so the large proton beam β - function, $\beta \sim d\,(N-1)$, and antiproton absorption in lithium on the length $\sim d\,(N-1)$ restrict the range of effective applicibility of such targetry scheme.

15

References

1. T.A.Vsevolozhskaya et al. The Antiproton Source for UNC IHEP. Contribution to VII All Union Conf. on Particle Accelerators, Dubna, October 14-16, 1980.

2. Design report. The Fermilab High-Intensity Antiproton Source, FNAL, October 1979.

3. B.F.Baianov et al. Proc. XI Int. Conf. on High Energy Accelerators, Geneva, CERN, 1980.

4. Beam Transport and Target System for pp and p$\bar{\text{p}}$ Colliding Beams, FNAL 06/20/78.

5. T.Vsevolozhskaya. The Chromatic Aberration of Lenses with Large Angular Acceptance, INP report 80-221, Novosibirsk,1980.

6. G.I.Budker, T.A.Vsevolozhskaya, G.I.Silvestrov, A.N.Skrinsky. Proc. of II All Union Conf. on Particle Accelerators, Moscow, vol. 2, 196 (1972).

7. H.Knoepfel. Pulsed High Magnetic Fields, London 1970.

8. V.M.Highdarov. The Installation for Study of the Possibility of Magnetic Field of 1-2 MG Production at Tangsten Rod Surface and the Rod Behaviour Study. Graduation Work, INP, 1968.

9. G.I.Budker, T.A.Vsevolozhskaya et al. Proc. of V All Union Conf. on Particle Acceleration, Moscow, vol. II, 299 (1977).

10. F.Binon et al. Phys. Lett. 30B, 506, 1969.

11. Yu.M.Antipov et al. Phys. Lett. 34B, 165, 1971.

12. N.I.Bozhko et al. IHEP report 79-78, Serpukhov, 1979.

13. L.M.Barkov et al. The Chanal for Intensive Secondary Particle Beams of Low Energy at PS of the IHEP. Contribution to VII All Union Conf. on Particle Accelerators, Dubna, October 14-16, 1980.
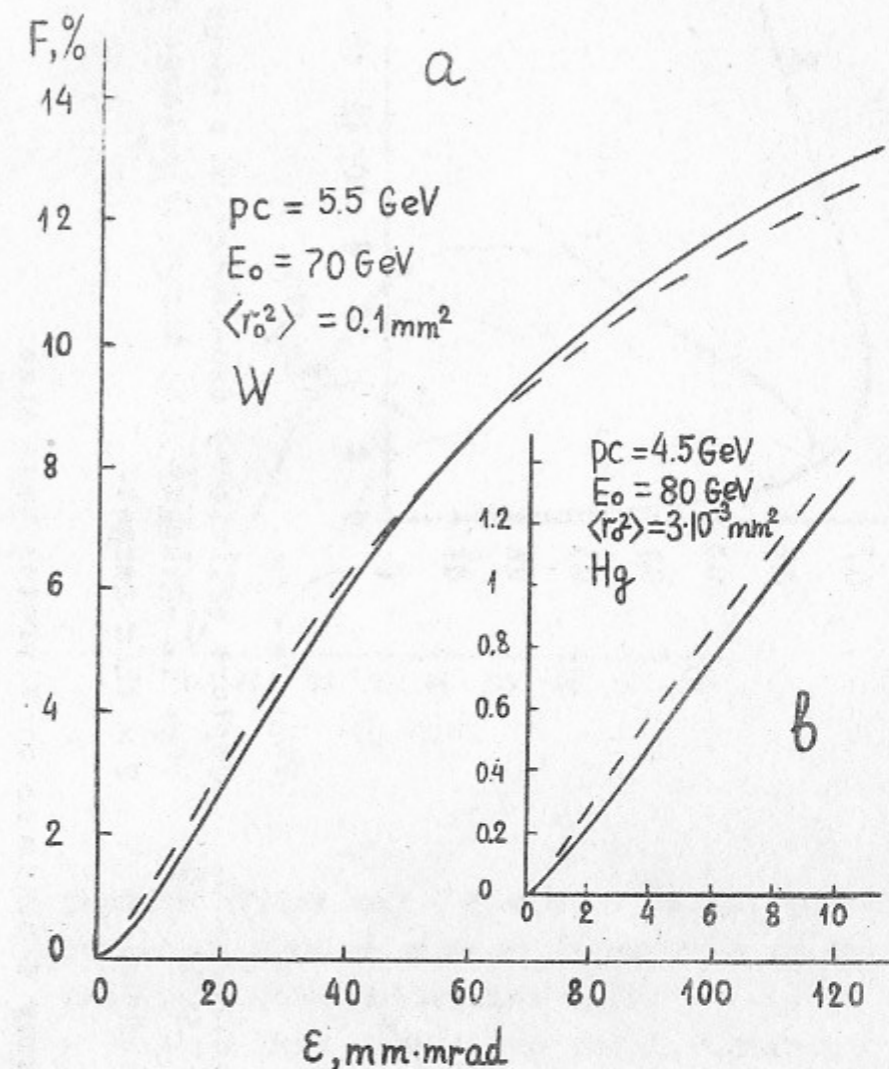
Fig. 1. Capture efficiency dependence on an acceptance value from computer simulation (solid lines) and equations (13) - (a) and (14) - (b) (dashed lines). Antiproton and proton momenta, mean square proton beam radius, and target material are written.
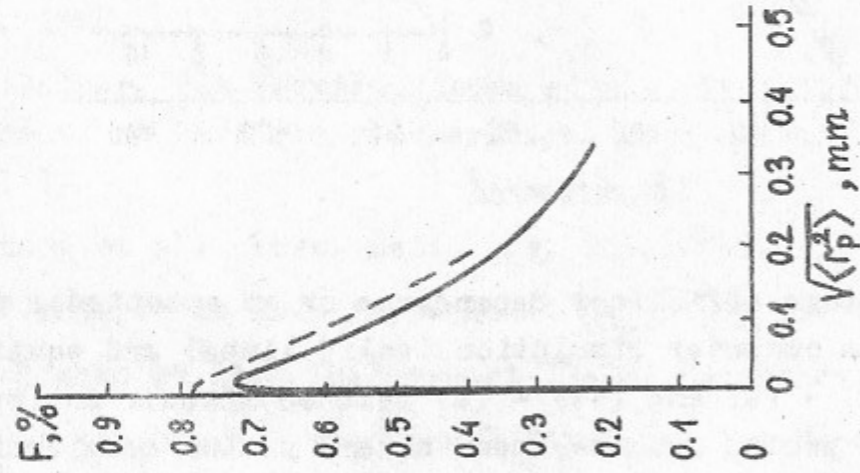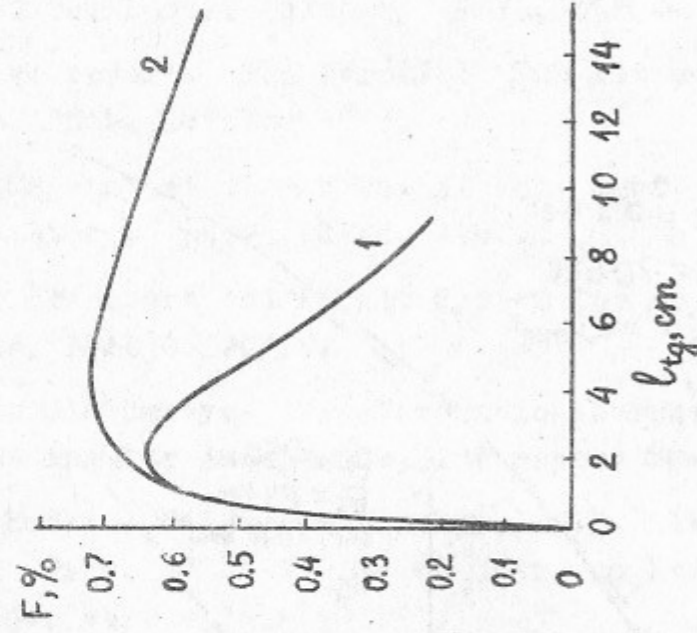
Fig. 3. Capture efficiency dependence on a target length for the: 1. – target with infinitely large cross-section, 2 – thin target.

Fig. 2. Capture efficiency dependence on a proton beam size from computer simulation (solid line) and eq. (14) (dashed line).
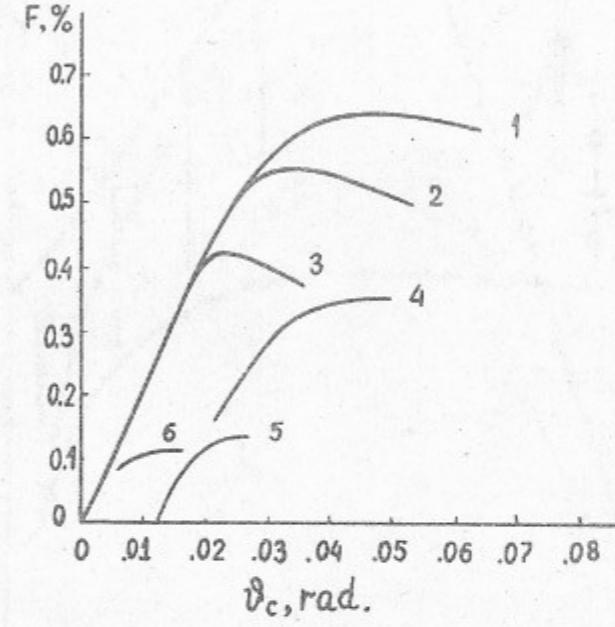

Fig. 4. Capture efficiency ($\varepsilon = 5 \cdot 10^{-6}$ mrad, pc = 4.5 GeV) versus an angular size of acceptance at the target under the antiproton collection with: 1 – ideal lens; 2 – – lithium lens with 10 cm focal distance f , 6 cm length l , $\emptyset$ 10 mm aperture, 2.5 mm end berillium flanges thickness Δ ; 3 – lithium lens with f = = 20 cm, l = 6 cm, $\emptyset$ 20 mm, Δ = 5 mm; 4 and 5 – linear parabolic lenses with f = 20 cm, 5 mm neck diameter, $\Delta(r) = \dfrac{5}{r(mm)}$ mm wall thickness, made of berillium and aluminium, respectively; 6 – quad triplet with $\sim$ 1 m lengths, $\sim$ 0.7 m drifts, $\sim$ 1 KOe/cm field gradient.
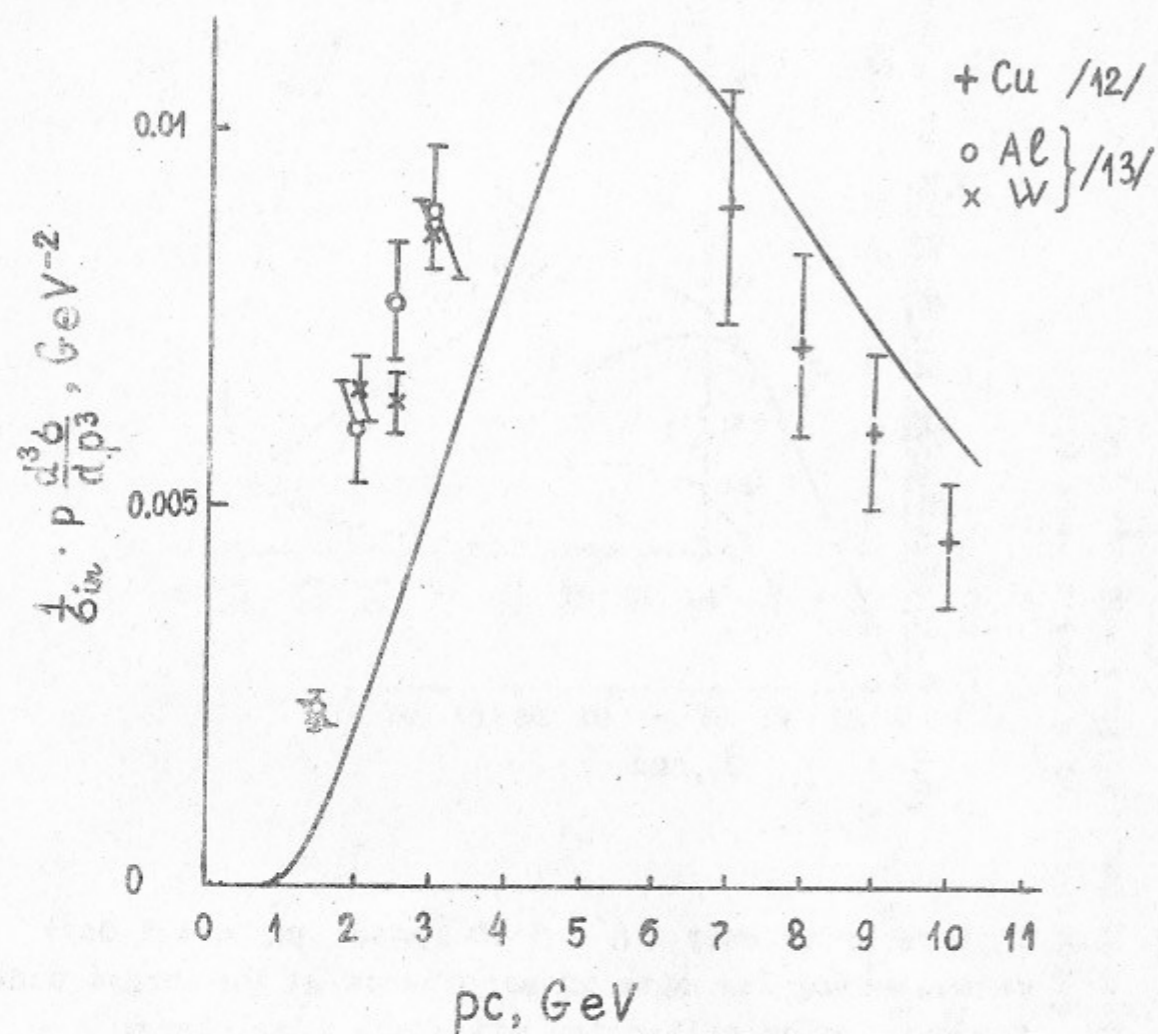
Fig. 5. Antiproton production cross-section versus a momentum.
Solid line - the data /10,11/, extrapolated to low
momenta under the simmetry of $E\frac{d^3\sigma}{dp^3}$ versus
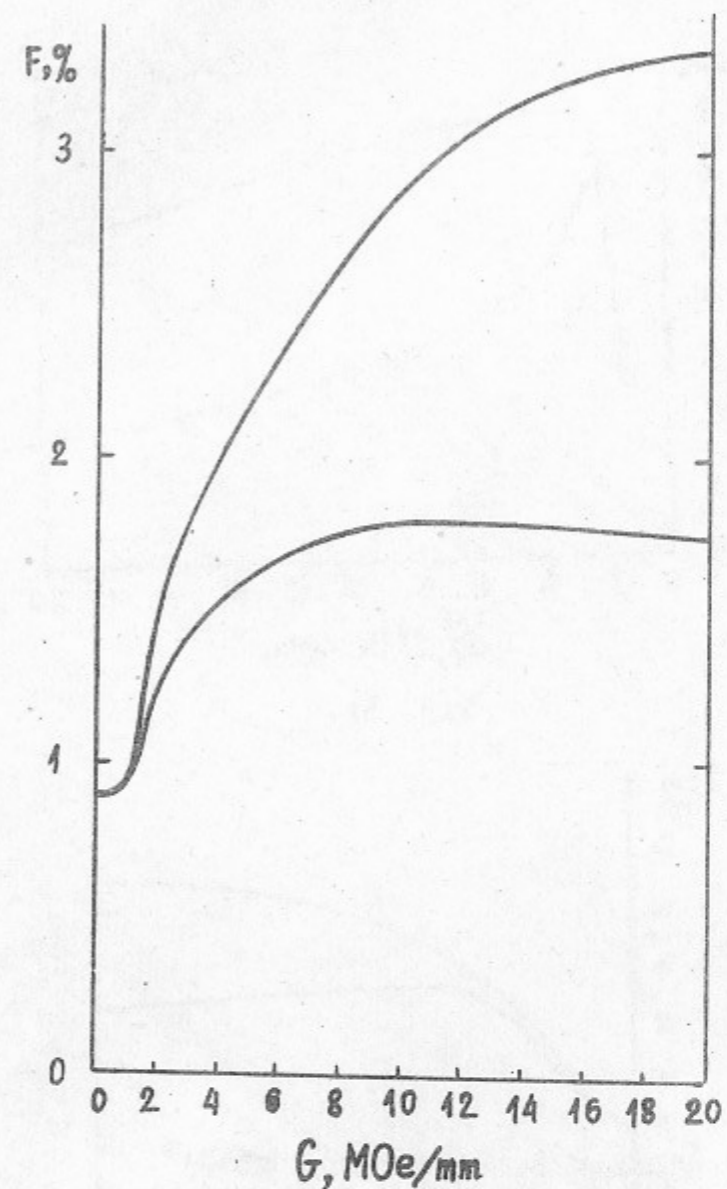c.m.s. rapidity; the points - data /12,13/.

Fig. 6a.

Fig. 6. Capture efficiency (a) and optimum target length (b)
dependence on a magnetic field gradient inside the
target for $5 \cdot 10^{-6}$ mrad acceptance ε , 4.5 GeV/c an-
tiproton momentum p , 80 GeV (1) and 800 GeV (2)
proton energies E_0 , $3 \cdot 10^{-3}$ mm² mean square spot ra-
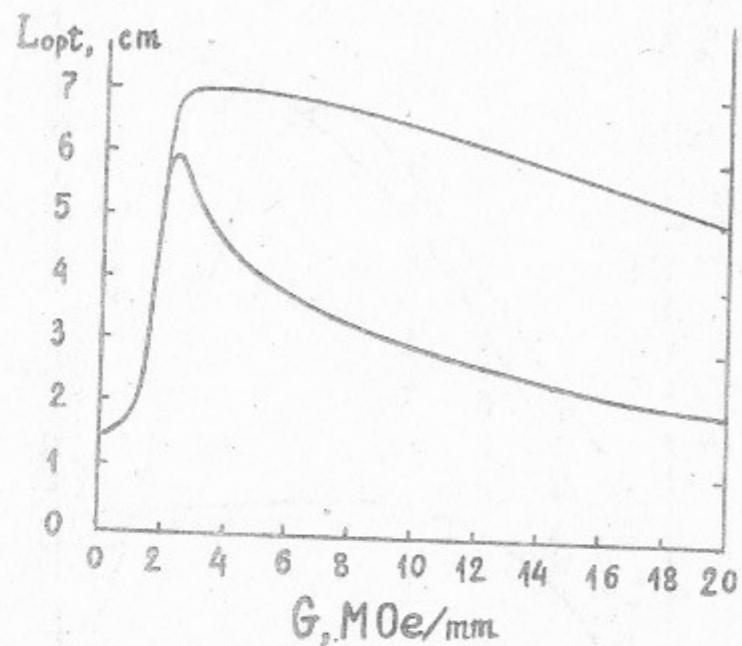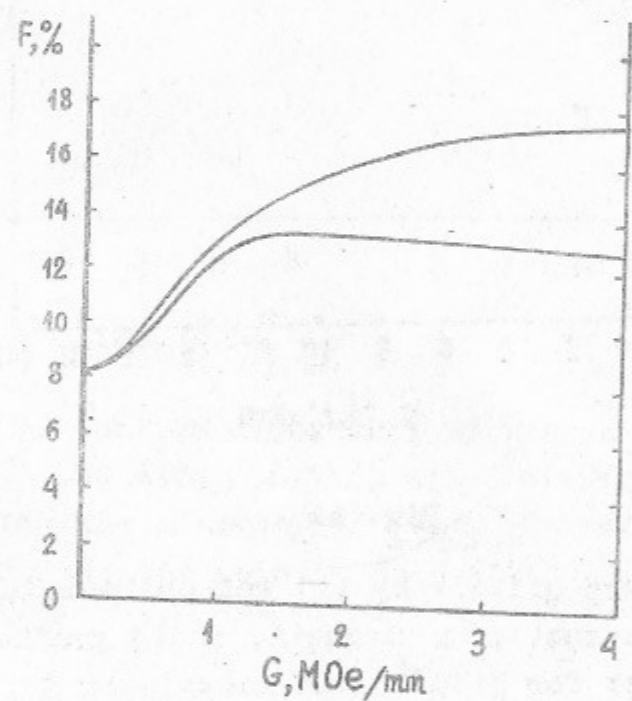dius $\langle r_0^2 \rangle$ the proton beam is focused in.

Fig. 6b.

Fig. 7. The same as in figure 6a for $\varepsilon = 6 \cdot 10^{-5}$ mrad,
$p = 5.5$ GeV/c , $E_0 = 70$ GeV (1) and 350 GeV (2),
$\langle r_0^2 \rangle = 0.1$ mm^2.